Theor Chem Acc (2005) 113: 42–57
DOI 10.1007/s00214-004-0603-2

Theoretical
Chemistry Accounts

Regular article

Redox potential of iron–sulfur clusters as a model of the *Desulfovibrio vulgaris* center

M. Czerwiński[1], **M. Matusiewicz**[2]

[1] Chemistry Institute, Pedagogical University, Al. Armii Krajowej 13/15, PL-42200, Częstochowa, Poland
[2] Institute of Computer Science, Technical University of Częstochowa, Al. Armii Krajowej 17, PL-42200, Częstochowa, Poland

Received: 5 February 2004 / Accepted: 25 May 2004 / Published online: 26 November 2004

Abstract. A theoretical study of Heisenberg exchange and double exchange effects in clusters with four and six iron ions has been performed for $[Fe_4S_3O]^{m+}$, $[Fe_4S_4]^{m+}$ (where $m=3$, 2), and $[Fe_6S_6]^{n+}$ (where $n=5$, 4) ions as models of the *Desulfovibrio vulgaris* iron–sulfur centers. Assuming that the redox potential mostly depends on the Heisenberg spin coupling and the resonance delocalization, we performed an analysis of the reduction process for the $[Fe_4S_3O]^{3+/2+}$, $[Fe_4S_4]^{3+/2+}$, and $[Fe_6S_6]^{5+/4+}$ ions and showed that the redox potential can be calculated as a difference between average spin energies of the tetravalent and pentavalent double cubane superclusters. For the Heisenberg parameter of $J_1=20$ cm^{-1}, the redox potential amounts to about 0.03 V. It complies with close to zero experimental values of the redox potential.

Keywords: Heisenberg exchange – Prismane – Double cubane – Hybrid cluster – Supercluster – Resonance delocalization

1 Introduction

Iron–sulfur clusters form a large class of structures that are important in metal cluster chemistry. Many types of the Fe–S clusters have recently been synthesized, structurally characterized and intensively investigated. A variety of synthetic methods have been proposed for preparation of compounds with desired properties, for example, the ox–redox potentials. Organometallic Fe–S clusters can be obtained by different methods, such as reactions of iron carbonyl complexes with sulfur-supplying agents, reactions of iron (II) salts and complexes with sulfides, or expansion of small clusters [1, 2, 3, 4]. On the other hand, Fe–S clusters have been observed in biological systems and play important roles in many biological processes. Such clusters of a mixed valence consisting of two, three, four, and six or more iron ions are involved in multi-electron-transfer processes or multi-electron-pair redox catalysis in proteins and complex enzymes. These processes are necessary for the activity of biological systems [5, 6, 7].

The available experimental data are difficult to interpret. The analysisis mainly based on electron paramagnetic resonance (EPR) spectroscopy, Mössbauer spectroscopy, magnetic circular dichroism spectroscopy, potentiometric methods as well as resonance Raman spectroscopy. For example, there are divergences in qualification of the geometry and the size of the cluster (number of iron ions and kind of bridge ions) in proteins from *Desulfovibrio vulgaris*. On the basis of the EPR spectroscopy analysis, it was hypothesized that the Fe–S clusters in these proteins are of ''prismane'' type [8].

The new crystal structure of the isolated ''prismane protein'' from *D. vulgaris* was determined in 1998 using an X-ray method (with a resolution of 1.72 Å). It was found that the protein does not contain the [Fe6S6] prismane cluster (as previously published [8]) but two 4Fe clusters [9], i.e., cluster 1 (cubane $[Fe_4S_4]$) and cluster 2 (the novel 4Fe ''hybrid'' cluster). The latter consists of two μ_2-sulfido-bridges, two μ_2-oxo-bridges, and a partially μ_2 bridged *X*. *X* represents a site whose precise nature has not been defined, but which may contain a disordered substrate molecule. This ''open'' structure suggests that it could be a site of catalytic activity. In conclusion, the authors of the work ascertained that ''resonance Raman spectroscopy suggests that the bridging ligand *X*, which could not be identified unambiguously in the crystal structure, is a solvent-exchangeable oxygen''.

Electronic Supplementary Material Supplementary material is available in the online version of this article at http://dx.doi.org/10.1007/s00214-004-0603-2.

Correspondence to: M. Czerwiński
e-mail: m.czerwinski@ajd.czest.pl

Our first theoretical papers [10, 11, 12, 13, 14] appeared nearly a decade ago and presented an interpretation of the EPR data for the Fe–S systems. The ambiguity of the structure of the *D. vulgaris* active center may result from the too low resolution of the X-ray method, as well as from the fact that different experimental methods examine the system in different ways and conditions. Therefore, the geometry of the active protein center can seem to be different. For all these reasons, theoretical examinations are necessary to determine changes in the geometry of these centers depending on number of iron ions and their valence obtained from experimental data other than EPR, for example, from electrochemical research (the ox–redox characteristics). For the cluster of the high-potential iron protein (HiPIP) type having a total spin of $S = 0$ and $1/2$ in the ground state, the experimental EPR data show the redox potential E_m $(4+/5+)$ has value of $+5$ mV [9, 15]. The experimental data were confirmed by our theoretical investigations.

2 Theoretical models

The proposed theoretical considerations based on the spin Hamiltonian allow us to calculate values of the total spin for the ground state (comparable with the values obtained using EPR) and the values of the redox potentials. We have introduced a model of spin interactions for the hybrid $[Fe_4S_3O]$ and the cubane $[Fe_4S_4]$ geometry as well as $[Fe_6S_6]$ of the prismane and double cubane $[Fe_6S_6]$ geometry to describe the Fe–S center in *D. vulgaris*. Although the center of *D. vulgaris* is probably composed of two 4Fe clusters, we have assumed that it is sufficient to examine the system with six iron ions describing the coupling of an additional two iron ions with the cluster of four ions. We will also discuss the influence on the redox potential, the spin configurations of the clusters (low and high spin) and delocalization of electrons.

Assuming a given cluster geometry, one obtains a Heisenberg Hamiltonian, which can be transformed in order to calculate the energy of the spin states. Calculation of matrix elements requires appropriate *n-j* Wigner symbols (e.g., 6-*j* in the case of the systems with three ions and 12-*j* for tetramers with delocalization of one electron). The Wigner symbols of 9-*j* type are defined through algebraic formulas that are convenient for numerical calculations, and are determined within the quantum theory of the angular momentum. Models connected with the spin interactions in real three-dimensional space and connected with a spin algebra for systems consisting of more than four metal ions were not developed until the middle of the 1990s, when our first publications, later publications of the Bencini group appeared. Other publications of Coropceanu et al. [16], Bencini et al. [17], and Borras et al. [18] presented special calculations for three- and four-center clusters.

While changing the cluster structure, a change of the spin Hamiltonian arises depending on the number and the value of the Heisenberg exchange parameters J_i and the values of the double-exchange b parameter. These parameters depend on the cluster type as well as on the ion type (and its valence) and the vibrational state of the system. A very important issue is to determine possible relationships between the Heisenberg J_i parameters, i.e., oscillation frequency, force constant of bonds, transfer parameters [19]. In the Fe–S clusters showing the same distance between the iron ions, the highest absolute value is reached by the exchange parameter J_1 describing Fe(III)–Fe(III) coupling, the exchange parameter describing Fe(III)–Fe(II) coupling has a lower absolute value, and the exchange parameter describing Fe(II)–Fe(II) coupling has the lowest absolute value [20, 21, 22, 23]. The values of the Heisenberg exchange parameters decrease considerably when the distance between the iron ions increases.

Here, we present our approach to calculations of the redox potential using spin state energies as a model. The analytical form of the matrix elements of the spin Hamiltonian is very complicated [16, 18]. By applying intermediate basis sets and uncoupling of spins, the spin Hamiltonian could be simplified to have Wigner symbols not higher than 9-*j*. In such a way, correlations have been introduced between the matrix elements of the spin Hamiltonian for the model systems consisting of four iron ions (hybrid and cubane) and six iron ions (prismane and double cubane). Comparison of the results for numerically calculated spin state energies and average energies of spin states for these structures allows us to discuss the influence of the geometry change and the number of iron ions and their valence on magnetic and ox–redox properties of iron clusters modeling the active center of *D. vulgaris*.

We will use our previous results for the model cluster of prismane and double cubane geometry [24, 25, 26]. Therefore, we introduced additional expressions describing the spin energy – with single exchange – elements $\hat{H}_{const}$, which depend on the exchange parameters and the squares of appropriate intermediate spins. Numerical calculations of the spin interactions were performed using our own HMVC package [27].

2.1 Spin Hamiltonian of the $[Fe_4S_3O]$ and the $[Fe_4S_4]$ systems for the hybrid and the cubane clusters

We will introduce the theoretical models for the $[Fe_4S_3O]^{3+}$ and $[Fe_4S_3O]^{2+}$ clusters (the active center of *D. vulgaris*) describing the hybrid system which has been recently determined using X-ray examinations [9] as well as for the $[Fe_4S_4]^{3+}$ and $[Fe_4S_4]^{2+}$ clusters of cubane type. These structures were theoretically examined by other authors as well [28, 29]. We present the most essential theory adjusted for numerical calculations of the spin energies (the remaining necessary formulas are in the Supporting Information available in the Electronic Supplementary Material, ESM).

2.1.1 Model for the hybrid system

A suitable electron configuration of $3d^5$ and $3d^6$ is expected for the Fe(III) and Fe(II) ions, respectively. We assumed the spin numbers $S_1 = S_2 = S_3 = 5/2$ and $S_4 = 2$ for $[Fe_4S_3\,O]^{3+}$ and $S_1 = S_2 = 5/2$, $S_3 = 2$, and $S_4 = 2$ for $[Fe_4S_3\,O]^{2+}$ (Fig. 1a) and the following relationships for Heisenberg parameters: $J = J_2 \geq J_1 \geq J_3 > J_4 > J_5 \geq J_6$. The values of the parameters in the following table were used:

Parameter	$J_{23} = J_1$	$J_{12} = J_2$	$J_{13} = J_3$	$J_{34} = J_4$	$J_{14} = J_5$	$J_{24} = J_6$
Value	J_1	(0.4–1.5)J_1	(0.4–1.5)J_1	$0.4J_1$	$0.1J_1$	$0.1J_1$

We introduced additionally relative parameters: $\alpha_1 = J_{12}/J_{23}$ and $\alpha_2 = J_{13}/J_{23}$.

The Heisenberg Hamiltonian for the hybrid system can be written as a general Hamiltonian for four interacting spins:

$$\hat{H} = J_1\hat{S}_2\hat{S}_3 + J_2\hat{S}_1\hat{S}_2 + J_3\hat{S}_1\hat{S}_3 + J_4\hat{S}_1\hat{S}_4 + J_5\hat{S}_2\hat{S}_4 + J_6\hat{S}_3\hat{S}_4. \quad (1)$$

2.1.2 Models for the cubane system

For the $[Fe_4S_4]^{3+}$ cluster of the cubane structure (Fig. 1b) we assumed that the following values of the spin numbers can be associated with each iron site: $S_1 = S_2 = S_3 = 5/2$ and $S_4 = 2$. With respect to symmetry and ion type,the following relations between the Heisenberg parameters occur: $J_{12} = J_{23} = J_{13} = J_2$ and $J_{14} = J_{24} = J_{34} = J_1$. This allows us to introduce only one parameter: $\alpha_1 = J_2/J_1$.

The Heisenberg Hamiltonian for the cubane structure looks as follows:

$$\hat{H} = J_1\left(\hat{S}_1\hat{S}_4 + \hat{S}_2\hat{S}_4 + \hat{S}_3\hat{S}_4\right) + J_2\left(\hat{S}_1\hat{S}_2 + \hat{S}_1\hat{S}_3 + \hat{S}_2\hat{S}_3\right). \quad (2)$$

The mechanism of the resonance delocalization consists in electron hopping between neighboring ions with nonzero spin. It can be noticed that there are four equivalent sites for one Fe(II) ion. We introduce a basis set consisting of four spin functions $\psi^1_{E_h}(S)$, $\psi^2_{E_h}(S)$, $\psi^3_{E_h}(S)$, and $\psi^4_{E_h}(S)$, where the upper index denotes the site number of the Fe(II) ion. Transition from one site to the other consists in hopping of one electron. All spin functions are equivalent. Let us consider the hopping between ions 2 and 4.

The resonance delocalization energy takes the following form:

$$E_d = \sum_{i=i(S_{13},S_{24})} c_i^2(S_{13},S_{24})\, b_1\left(S_{24} + 1/2\right). \quad (3)$$

Solving Eq. (4), we get the total energy E_t:

$$\det\begin{pmatrix} E - E_t & E_d & E_d & E_d \\ E_d & E - E_t & E_d & E_d \\ E_d & E_d & E - E_t & E_d \\ E_d & E_d & E_d & E - E_t \end{pmatrix} = 0. \quad (4)$$

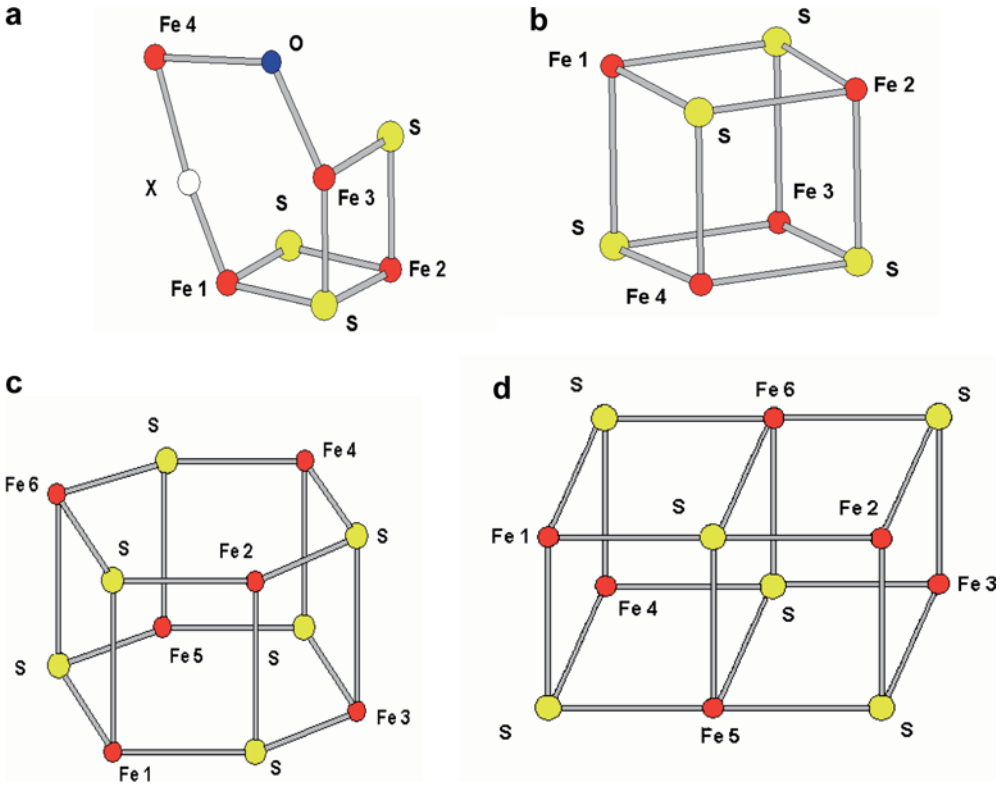

Fig. 1 Structures of the clusters: **a** hybrid structure of Fe_4S_3O X cluster, where X is unknown; **b** idealized cubane structure of the Fe_4S_4 cluster; **c** prismane structure of the $Fe_6S_6X_6$ supercluster, where X is Cl, Br, or I; **d** idealized double cubane structure of the Fe_6S_6 supercluster

For the $[Fe_4S_4]^{2+}$ cluster (of cubane structure, Fig. 1b) we assume $S_1 = S_2 = 5/2$ and $S_3 = S_4 = 2$, and for the $[Fe_4S_4]^{3+}$ cluster we assume that the values of the spin numbers that can be associated with each iron site: $S_1 = S_2 = S_3 = 5/2$ and $S_4 = 2$, and in respect of symmetry and the type of ions the following relations between the Heisenberg parameters occur: $J_{13} = J_{23} = J_{14} = J_{24} = J_1$, $J_{12} = J_2$, and $J_{34} = J_3$ (in our numerical calculations $J_{34} = 0.8J_1$). Let us introduce two dimensionless parameters $\alpha_1 = J_2/J_1$ and $\alpha_2 = J_3/J_1$ to describe the diagrams.

$$\hat{H} = J_1\left(\hat{S}_1\hat{S}_3 + \hat{S}_1\hat{S}_4 + \hat{S}_2\hat{S}_3 + \hat{S}_2\hat{S}_4\right) + J_2\hat{S}_1\hat{S}_2 + J_3\hat{S}_3\hat{S}_4 \qquad (5)$$

There are six equivalent sites of two Fe(II) ions. In order to describe the resonance delocalization let us introduce the basis composed of six spin functions: $\psi^{12}_{E_h}(S)$, $\psi^{13}_{E_h}(S)$, $\psi^{14}_{E_h}(S)$, $\psi^{23}_{E_h}(S)$, $\psi^{24}_{E_h}(S)$, and $\psi^{34}_{E_h}(S)$, where the upper indexes denote the sites of Fe(II) ions. Transitions from one site to another consist in hopping of one or more electrons. All one-electron transitions are equivalent. Similarly to $[Fe_4S_4]^{3+}$, let us consider hopping between ions 2 and ion 4. Then,

$$E_{d1} = \sum_{i=i(S_{13},S_{24})} c_i^2(S_{13},S_{24})b_1\left(S_{24} + 1/2\right). \qquad (6)$$

All two-electron transitions are also equivalent. Let us consider simultaneous hopping between ions 2 and 4 as well as between ions 1 and 3. Then,

$$E_{d2} = \sum_{i=i(S_{24},S_{13})} c_i^2(S_{24},S_{13})b_2\left(S_{24} + 1/2\right)\left(S_{13} + 1/2\right). \qquad (7)$$

Let us introduce two double exchange parameters b_1 and b_2. Solving the equation

$$\det\begin{pmatrix} E-E_t & E_{d1} & E_{d1} & E_{d1} & E_{d1} & E_{d2} \\ E_{d1} & E-E_t & E_{d1} & E_{d1} & E_{d2} & E_{d1} \\ E_{d1} & E_{d1} & E-E_t & E_{d2} & E_{d1} & E_{d1} \\ E_{d1} & E_{d1} & E_{d2} & E-E_t & E_{d1} & E_{d1} \\ E_{d1} & E_{d2} & E_{d1} & E_{d1} & E-E_t & E_{d1} \\ E_{d2} & E_{d1} & E_{d1} & E_{d1} & E_{d1} & E-E_t \end{pmatrix} = 0, \qquad (8)$$

we obtain the total energy E_t.

If we have the spin energies, we can calculate the average spin energy as a function of temperature T (Eq. 9):

$$E_{average} = \frac{\sum_{i-\text{all spin states}} E_i(S)D_i(S)\exp\left(-\frac{E_i(S)}{kT}\right)}{\sum_{i-\text{all spin states}} D_i(S)\exp\left(-\frac{E_i(S)}{kT}\right)}. \qquad (9)$$

The zero-point-energy (ZPE) reference for the spin-coupled systems has been defined as the spin barycenter energy (Eq. 10) of the spin ladder [30]. The spin barycenter energy must be considered both for the reduced form and for the oxidized form, while calculating the redox potential, when we determine it from the difference of the appropriate ground spin state energies:

$$E_{barycenter} = \frac{\sum_{i-\text{all spin states}} E_i(S)D_i(S)}{\sum_{i-\text{all spin states}} D_i(S)}, \qquad (10)$$

where $D_i(S) = 2S + 1$ – the degeneration number of the ith spin state—and $E_i(S)$ is the energy of the ith spin state.

2.2 Heisenberg Hamiltonian of the [Fe6S6] system with resonance delocalization for the prismane and the double cubane clusters

For each of the clusters (of a specified geometry) we assume two different charges, which requires to introduce a separate spin model (with respect to different forms of resonance delocalization). Further, we describe in detail the model for the $[Fe_6S_6]^{5+}$ prismane system because it is published for the first time, whereas for the $[Fe_6S_6]^{4+}$ prismane and double cubane systems key issues will be mentioned to keep this publication readable (more details were included in our previous publications [24, 25, 26]).

2.2.1 Model for the prismane system

The Heisenberg Hamiltonian for the $[Fe_6S_6]^{5+}$ prismane system presented in Fig. 1c can be written as:

$$\begin{aligned}\hat{H} = {} & J_1\left(\hat{S}_1\hat{S}_6 + \hat{S}_5\hat{S}_6\right) + J_2\left(\hat{S}_1\hat{S}_2 + \hat{S}_2\hat{S}_3 + \hat{S}_3\hat{S}_4 + \hat{S}_4\hat{S}_5\right) \\ & + J_3\left(\hat{S}_2\hat{S}_6 + \hat{S}_4\hat{S}_6\right) + J_4\left(\hat{S}_1\hat{S}_3 + \hat{S}_3\hat{S}_5 + \hat{S}_1\hat{S}_4 + \hat{S}_2\hat{S}_4\right) \\ & + J_5\hat{S}_3\hat{S}_6 + J_6\left(\hat{S}_1\hat{S}_4 + \hat{S}_2\hat{S}_5\right), \end{aligned} \qquad (11)$$

where J_i is one of the Heisenberg exchange parameters. A suitable electron configuration of $3d^5$ and $3d^6$ is expected for the Fe(III) and the Fe(II) ions, respectively; thus $S_1 = S_2 = S_3 = S_4 = S_5 = 5/2$ and $S_6 = 2$.

The resonance delocalization can take place in systems of mixed valence. Since we have one Fe(II) ion in the$[Fe_6S_6]^{5+}$ system investigated, the ion can be observed in any position, always leading to the same Heisenberg–Dirac–van Vleck (HDVV) Hamiltonian. In this case, the delocalization of a missing electron should be introduced for all six-iron ions. The wave function can be written as:

$$\Psi = a_1\psi_1 + a_2\psi_2 + a_3\psi_3 + a_4\psi_4 + a_5\psi_5 + a_6\psi_6, \qquad (12)$$

where ψ_i is an eigenfunction of the HDVV type and the Fe(II) ion is located in the ith position. Because of the system symmetry, the function ψ_i will be the same for each "i" position. In the case of the Fe–Fe distance, we

can distinguish electron transfer of three types. The first one is between the nearest neighbors, i.e., 1:2 and 2:3, d_1 distance. The second type can be observed between ions localized at hexagon corners, i.e., 1:3 and 2:4, d_2 distance, and the third type is between the most distant ions, i.e., 1:4, 2:5, and 3:6, d_3 distance.

Let us define $\hat{H}_{\mathrm{d}}$ as the Hamiltonian containing the electron transfer operators as described in our previous publication [25]:

$$\begin{aligned}\hat{H}_{\mathrm{d}} = {} & b_1(d_1)\left[\hat{T}_{12}+\hat{T}_{23}+\hat{T}_{34}+\hat{T}_{45}+\hat{T}_{56}+\hat{T}_{61}\right] \\ & +b_2(d_2)\left[\hat{T}_{13}+\hat{T}_{24}+\hat{T}_{35}+\hat{T}_{46}+\hat{T}_{51}+\hat{T}_{62}\right] \\ & +b_3(d_3)\left[\hat{T}_{14}+\hat{T}_{25}+\hat{T}_{36}\right],\end{aligned} \tag{13}$$

where

$$\hat{T}_{ij}|\varphi_{\mathrm{d}}\rangle_k = \left(\delta_{ik}|\varphi_{\mathrm{d}}\rangle_i + \delta_{jk}|\varphi_{\mathrm{d}}\rangle_j\right)\left(S_{ij}+1/2\right) \tag{14}$$

and

$$|\varphi_{\mathrm{d}}\rangle = |S_1 S_6(S_{16}) S_5(S_{156}) S_2 S_4(S_{24}) S_3(S_{234}) S\rangle. \tag{15}$$

Here $|\varphi_{\mathrm{d}}>_{\mathrm{k}}$ is a base vector with a defied number S_{ij}. The index outside the brackets means that the Fe(II) ion is located at the k-th point, and δ_{ij} is a Kronecker delta. The parameter b_i (double exchange) depends above all on the distance d_i .

The total Hamiltonian can be expressed as follows:

$$\hat{H}_{\mathrm{total}} = \sum_i \hat{H}_i + \hat{H}_{\mathrm{d}}, \tag{16}$$

where $\hat{H}_i$ is a HDVV operator that acts on the ψ_i state only.

In order to find the energy associated with the spin interactions and described by the Hamiltonian (Eq. 16), the following equation should be solved:

$$\hat{H}_{\mathrm{total}}\Psi = E_{\mathrm{total}}\Psi. \tag{17}$$

In matrix form, it is expressed as follows:

$$\det\begin{Bmatrix} E-E_{\mathrm{total}} & E_{\mathrm{d1}} & E_{\mathrm{d2}} & E_{\mathrm{d3}} & E_{\mathrm{d2}} & E_{\mathrm{d1}} \\ E_{\mathrm{d1}} & E-E_{\mathrm{total}} & E_{\mathrm{d1}} & E_{\mathrm{d2}} & E_{\mathrm{d3}} & E_{\mathrm{d2}} \\ E_{\mathrm{d2}} & E_{\mathrm{d1}} & E-E_{\mathrm{total}} & E_{\mathrm{d1}} & E_{\mathrm{d2}} & E_{\mathrm{d3}} \\ E_{\mathrm{d3}} & E_{\mathrm{d2}} & E_{\mathrm{d1}} & \mathrm{E}-\mathrm{E}_{\mathrm{total}} & E_{\mathrm{d1}} & E_{\mathrm{d2}} \\ E_{\mathrm{d2}} & E_{\mathrm{d3}} & E_{\mathrm{d2}} & E_{\mathrm{d1}} & E-E_{\mathrm{total}} & E_{\mathrm{d1}} \\ E_{\mathrm{d1}} & E_{\mathrm{d2}} & E_{\mathrm{d3}} & E_{\mathrm{d2}} & E_{\mathrm{d1}} & E-E_{\mathrm{total}} \end{Bmatrix} = 0 \tag{18}$$

where $E_{\mathrm{d}i} = \sum_{\mathrm{k}} c^2(\mathrm{k})\left[{}_m\langle\varphi_{\mathrm{d}}|b_i(d_i)\hat{T}_{m\ n}|\varphi_{\mathrm{d}}\rangle_n\right]\left(S_{m\ n}+1/2\right)$ and $c(k)$ are expansion coefficients with k numbering ϕ_{d} states.

The φ_0 function (eigenfunction of the Hamiltonian $\hat{H}_0$, see Eq. 47) is expressed by the φ_{d} one:

$$\begin{aligned}&|(S_{15})(S_{135})(S_{24})(S_{246})S\rangle \\ &\quad = \sum_{S_{16}}\sum_{S_{156}S_{234}} |(S_{16})(S_{156})(S_{24})(S_{234})S\rangle \\ &\qquad \times \langle(S_{16})(S_{156})(S_{24})(S_{234})S \mid (S_{15})(S_{156})(S_{24})(S_{234})S\rangle \\ &\qquad \times\langle(S_{15})(S_{156})(S_{24})(S_{234})S \mid (S_{15})(S_{135})(S_{24})(S_{246})S\rangle,\end{aligned} \tag{19}$$

where

$$\begin{aligned}&\langle(S_{16})(S_{156})(S_{24})(S_{234})S \mid (S_{15})(S_{156})(S_{24})(S_{234})S\rangle \\ &\quad = (-1)^{S_5+S_6+S_{15}+S_{16}}\left[(2S_{15}+1)(2S_{16}+1)\right]^{1/2} \\ &\qquad \times \begin{Bmatrix} S_5 & S_1 & S_{15} \\ S_6 & S_{156} & S_{16}\end{Bmatrix}\end{aligned} \tag{20}$$

and

$$\begin{aligned}&\langle(S_{15})(S_{156})(S_{24})(S_{234})S \mid (S_{15})(S_{135})(S_{24})(S_{246})S\rangle \\ &\quad = \left[(2S_{135}+1)(2S_{246}+1)(2S_{156}+1)(2S_{234}+1)\right]^{1/2} \\ &\qquad \times \begin{Bmatrix} S_{15} & S_3 & S_{135} \\ S_6 & S_{24} & S_{246} \\ S_{156} & S_{234} & S\end{Bmatrix}.\end{aligned} \tag{21}$$

The influence of the electron transfer parameters b_2 and b_3 on $\hat{H}_{\mathrm{d}}$ is negligible, since the values of these integrals and all the same extradiagonal matrix elements in Eq. (18) decrease rapidly with increasing distance between the iron ions. Therefore, we will investigate the influence of the resonance delocalization using one parameter (only E_{d1}) and we will assume zero values of the remaining E_{d2} and E_{d3} parameters.

For a Heisenberg Hamiltonian with the resonance delocalization for the $[Fe_6S_6]^{4+}$ prismane system with regard to a supercluster symmetry and electrostatic interactions, we assumed Fe(III) at points 1, 2, 5, and 6 and Fe(II) points 3 and 4.

Then the Heisenberg Hamiltonian looks as follows:

$$\hat{H} = J_1\left(\hat{S}_1\hat{S}_4 + \hat{S}_2\hat{S}_3 + \hat{S}_3\hat{S}_6 + \hat{S}_4\hat{S}_5\right) + J_2\left(\hat{S}_1\hat{S}_6 + \hat{S}_2\hat{S}_5\right) + J_3\left(\hat{S}_3\hat{S}_5 + \hat{S}_4\hat{S}_6 + \hat{S}_1\hat{S}_3 + \hat{S}_2\hat{S}_4\right) + J_4\left(\hat{S}_1\hat{S}_5 + \hat{S}_2\hat{S}_6\right) + J_5\left(\hat{S}_1\hat{S}_2 + \hat{S}_5\hat{S}_6\right) + J_6\hat{S}_3\hat{S}_4. \quad (22)$$

The total Hamiltonian, including the double exchange, takes the following form:

$$\hat{H}_t = \hat{H} + \hat{H}_d, \quad (23)$$

where

$$\hat{H}_d = \hat{H}_{d(1-4,2-3)} + \hat{H}_{d(1-6,2-5)} + \hat{H}_{d(3-6,4-5)} = b\left[\left(\hat{T}_{14} \circ \hat{T}_{23}\right) + \left(\hat{T}_{16} \circ \hat{T}_{25}\right) + \left(\hat{T}_{36} \circ \hat{T}_{45}\right)\right], \quad (24)$$

where $\hat{T}_{ij}$ denotes an electron hopping operator of the pair ij, it acts only if the pair possesses an extra electron. To obtain the eigenenergy of the Hamiltonian [42] one should solve a secular equation:

$$\det\begin{pmatrix} E - E_t & E_d & E_d \\ E_d & E - E_t & E_d \\ E_d & E_d & E - E_t \end{pmatrix} = 0, \quad (25)$$

where

$$E_d = \left\langle \psi^{12}_{E_k}(S)\middle|\hat{H}_{d(1-4,2-3)}\middle|\psi^{34}_{E_k}(S)\right\rangle = \left\langle \psi^{12}_{E_k}(S)\middle|\hat{H}_{d(1-6,2-5)}\middle|\psi^{56}_{E_k}(S)\right\rangle = \left\langle \psi^{34}_{E_k}(S)\middle|\hat{H}_{d(3-6,4-5)}\middle|\psi^{56}_{E_k}(S)\right\rangle. \quad (26)$$

Therefore the eigenfunction recorded with Eq. (26) can be denoted as

$$\psi_E(S) = \sum_{i=i(S_{14},S_{23},S_{56},S_{1234})} c_{iE}(S_{14}, S_{23}, S_{56}, S_{1234}) \times |S_1S_4(S_{14})S_2S_3(S_{23})(S_{1234})S_5S_6(S_{56})S\rangle. \quad (27)$$

2.2.2 Model for the double cubane system

For the supercluster $[Fe_6S_6]^{5+}$ of double cubane structure (Fig. 1d), we assume the following spin numbers: $S_1 = S_2 = S_3 = S_4 = S_5 = 5/2$ and $S_6 = 2$, and we can write the following equation for the Heisenberg Hamiltonian:

$$\hat{H} = J_1\left(\hat{S}_1 + \hat{S}_2 + \hat{S}_3 + \hat{S}_4 + \hat{S}_5\right)\hat{S}_6 + J_2\left(\hat{S}_1\hat{S}_4 + \hat{S}_1\hat{S}_5 + \hat{S}_2\hat{S}_3 + \hat{S}_3\hat{S}_5 + \hat{S}_2\hat{S}_5 + \hat{S}_4\hat{S}_5\right) + J_3\left(\hat{S}_1\hat{S}_2 + \hat{S}_3\hat{S}_4\right) + J_3\left(\hat{S}_1\hat{S}_3 + \hat{S}_2\hat{S}_4\right), \quad (28)$$

which is transformed to

$$\hat{H}_0 = {}^1\!/_2 J_1\left[\hat{S}^2 + (\alpha_1 - 1)\hat{S}^2_{12345} + (\alpha_3 - \alpha_1)\left(\hat{S}^2_{13} + \hat{S}^2_{24}\right)\right] + \hat{H}_{const} \quad (29)$$

and

$$\hat{H}_1 = {}^1\!/_2 J_1(\alpha_2 - \alpha_1)\left(\hat{S}^2_{12} + \hat{S}^2_{34}\right), \quad (30)$$

where

$$\hat{H}_{const} = {}^1\!/_2 J_1\left[-\hat{S}^2_6 + \alpha_1\left(\hat{S}^2_1 + \hat{S}^2_2 + \hat{S}^2_5 + \hat{S}^2_4 - \hat{S}^2_5\right) - (\alpha_2 + \alpha_3)\left(\hat{S}^2_1 + \hat{S}^2_2 + \hat{S}^2_5 + \hat{S}^2_4\right)\right]. \quad (31)$$

In order to obtain resonance delocalization, we consider two equivalent sites of one ion Fe(II)-points 5 and 6. Let us consider the hopping between ions 5 and 6.

Then, the delocalization energy is described by

$$E_d = \sum_d c^2(d)\left(S_{56} + {}^1\!/_2\right), \quad (32)$$

where $c(d)$ is an appropriate coefficient of the expansion of the eigenfunction for the resonance delocalization $\hat{H}_d$ in the base in which there is S_{56} spin; d numerates this basis set. We obtain the total energy E_t considering double exchange solving the following secular equation:

$$\det\begin{pmatrix} E - E_t & E_d \\ E_d & E - E_t \end{pmatrix} = 0. \quad (33)$$

For $[Fe_6S_6]^{4+}$ of double cubane geometry the Heisenberg Hamiltonian can be denoted as

$$\hat{H} = J_1\left[\left(\hat{S}_3 + \hat{S}_4\right)\left(\hat{S}_5 + \hat{S}_6\right) + \hat{S}_1\hat{S}_4 + \hat{S}_3\hat{S}_2\right] + J_2\left[\left(\hat{S}_1 + \hat{S}_2\right)\left(\hat{S}_5 + \hat{S}_6\right) + \hat{S}_5\hat{S}_6\right] + J_3\left(\hat{S}_1\hat{S}_3 + \hat{S}_2\hat{S}_4\right) + J_4\hat{S}_1\hat{S}_2 + J_5\hat{S}_3\hat{S}_4, \quad (34)$$

where $S_1 = S_2 = S_5 = S_6 = 2.5$ and $S_3 = S_4 = 2$.

The double exchange Hamiltonian can be written as

$$\hat{H}_d = b\left(\hat{T}_{14} \circ \hat{T}_{23}\right) \quad (35)$$

and the resonance energy can be denoted as

$$E_d = \left\langle \psi^B_{E_k}(S,S_{56})\middle|\hat{H}_d\middle|\psi^A_{E_k}(S,S_{56})\right\rangle = b\sum_{i=i(S_{14},S_{23},S_{1234})} c^2_{iE_k}(S_{14},S_{23},S_{1234}) \times \left(S_{14} + {}^1\!/_2\right)\left(S_{23} + {}^1\!/_2\right). \quad (36)$$

3 Redox potential for cluster models of the *D. vulgaris* center

It is worth emphasizing that the redox potential of the systems with metal ions also depends on the negative charge of the ligand that facilitates the occurrence of a metal ion in a higher oxidation state (the higher the negative charge, the lower the redox potential). It also depends on the reductive capacity (σ electron) of a ligand that stabilizes the high redox grades of a given metal ion, and on the oxidation capacity (π electron) of a ligand that stabilizes the low redox grades of a metal. Finally, the redox potential depends on the system structure (i.e., on the cluster geometry), which can be dependent on the redox grades of the metal ions and, above all, can fluctuate together with the spin value of the ground state of the system.

Calculations of the redox potentials for the Fe–S proteins, using *ab initio* and density functional theory methods, are very difficult. Until recently they have been too complex for systems comprising more than one metal ion. This situation changed in recent years. The density functional calculations appear to be able to determine the redox potentials in a more reliable waythan before [26, 29, 30, 31, 32]. However, for many Fe–S proteins the theoretical results are a few dozen percent higher than the experimental results. This is due to a number of reasons, above all to difficulties in determining the geometry (because of the complexity of the system and the occurrence of processes such as the formation of hydrogen bonds or the migration of protons). The description of the latter is rather difficult. In addition, some errors may occur in predictions of the response of a solvent or protein environment to a charge change in the system. Therefore, it is still important to look for methods that could facilitate modeling of ox–redox processes.

We will demonstrate our results obtained based on theoretical models. The redox potential can be presented as a sum of the redox potential vacuum term of the system in the absence of spin coupling, the Heisenberg spin coupling, the resonance delocalization, and the solvatation energy of the system [30, 31, 32, 33]. It has been shown for $[Fe_4S_4]$ systems that a relatively large part of this sum is associated with the electron–electron repulsion coupling, and the redox potential vacuum term is almost completely compensated by the solvation term. This causes a dependence of the redox potential mostly on the Heisenberg spin coupling and the resonance delocalization. We calculated the redox potential assuming the previously mentioned data and using the theoretical models (introduced in Sect. 2) for the geometry of the clusters – prismane and double cubane for $[Fe_6S_6]$ systems and hybrid or cubane for $[Fe_4S_3O]$ and $[Fe_4S_4]$ systems. Thereafter we will discuss the possible influence of the cluster geometry and resonance delocalization on the value of the redox potential. This can be considered in the framework of the spin Hamiltonian for an appropriate selection of the Heisenberg J_i and double exchange b parameters (index i determines the number of these parameters as a result of the model applied).

The redox potential of the $[Fe_6S_6]^{5+/4+}$ or $[Fe_4S_4]^{3+/2+}$ system can be calculated as a difference in the energy of the states for $[Fe_6S_6]^{5+}$ and $[Fe_6S_6]^{4+}$ or $[Fe_4S_4]^{3+}$ and $[Fe_4S_4]^{2+}$, respectively. Analysis of the numerical results in a graphical form and in tables can be performed to demonstrate which clusters can be theoretically responsible for the actual redox process.

3.1 Results of calculations for the redox potential of the [Fe₄S₃O] and the [Fe₄S₄] systems

The results of numerical calculations for the spin state energy for the hybrid and cubane structures are presented in Figs. 2, 3, 4, and 5, ESM, Figs. 1–13, and Table 1. Changes in the number of iron ions or in the cluster structure influence not only the form of the spin Hamiltonian but also the number and the values of the Heisenberg J_i parameters and the values of the double exchange parameters b.

For the $[Fe_4S_3O]$ and the $[Fe_4S_4]$ systems, we assumed similar relations between the Heisenberg parameters as those for the systems with six iron ions. Spin state energies depending on the parameter α_1 are presented in Fig. 2 and ESM Figs. 1 and 2 for the hybrid cluster (charge of $+2$ and $+3$) showing a linear function of this parameter in the whole area, connected with the HiPIP nature of the system. Moreover, these diagrams of energy states are reciprocally parallel. The ground states for the systems show the lowest multiplicity for the hybrid cluster $[Fe_4S_3O]^{3+}$ (ESM, Fig. 2). These two states $S=0.5$ and 1.5 are situated very close to each other, and higher states are well separated together with the increasing total spin. In the case of the $[Fe_4S_3O]^{2+}$ hybrid cluster (ESM, Fig. 1), the situation is very similar, except for the accidental degeneracy, and the ground state (with $S=0$) is well separated from the spin ($S=1$) state. The sequence of the spin states is compliant with the order set of the increasing total spin.

This picture does not change on changing the cluster geometry (Fig. 3, ESM, Figs. 3 and 4) to the cubane one for compounds with charges $+3$ and $+2$, except for the differences in the energy. The corresponding states (of the same total spin) for clusters of the cubane geometry are located below the states determined for the clusters with hybrid geometry. The use of the double exchange (ESM, Figs. 5 and 6) results in shifting all the states without changing the order of their energy. Therefore, the resonance delocalization additionally stabilizes these systems. Other parameters (i.e., α_2 and α_3) have rather a slight influence on the energies and undoubtedly do not change the energy order of the spin states.

Therefore, for the $[Fe_4S_4]^{3+}$ and the $[Fe_4S_4]^{2+}$ clusters the calculated spin values for the ground state are

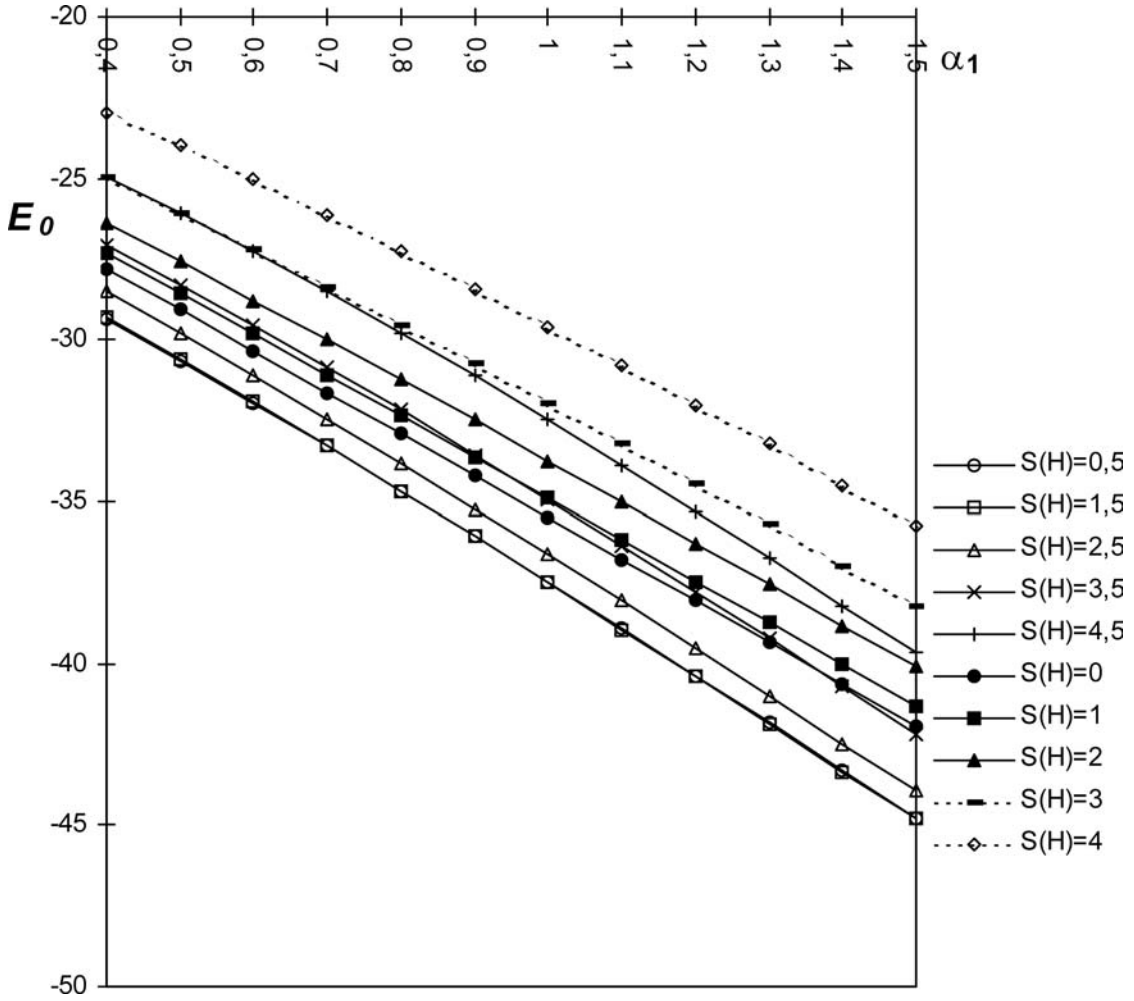

Fig. 2 Energy levels of a few of the lowest states (without resonance delocalization) in relation to the parameter α_1. The *continuous line* marks the states for $[Fe_4S_4]^{3+}$ and $[Fe_4S_4]^{2+}$, for the hybrid structure.

consistent with the experimental EPR data for the synthetic HiPIP-type clusters and clusters built into biological systems [34, 35].

A few of the lowest states for the systems with charge $+3$ and $+2$ are presented for the hybrid structures and for cubane ones in Figs. 2, 3, and, ESM Fig. 7. In the region where $\alpha_1 > 1.0$ (typical for the HiPIP systems) we can observe significant differences connected with the structure of these clusters. By presenting the chosen (substantial) lowest spin states in Figs. 2 and 3 for hybrid clusters of $+3$ and $+2$ ions, we demonstrate that the states of $S = 0.5$, 1.5, and 2.5 are located below the corresponding three lowest states for the $[Fe_4S_4]^{2+}$ ion. An inverse order can be observed for the cubane structure. The analysis of Fig. 3 and ESM, Fig. 7 shows that independently of whether the resonance delocalization is considered or not, the spin states for the $[Fe_4S_4]^{3+}$ ion are located below the corresponding states for $[Fe_4S_4]^{2+}$. Comparing the location of the few lowest spin energy levels for all structures considered for the $[Fe_4S_4]^{3+}$ and $[Fe_4S_4]^{2+}$ systems, one can observe the energy levels for the cubane structure are significantly below (around 20 J_1) the levels for the hybrid ones. Therefore, for the assumed number of four iron ions, the reduction process should occur in the states for the hybrid structure. The redox potential calculated as a difference in the energies of the ground spin states (with ΔZPE) for the $+3$ and $+2$ clusters is negative (-0.1 V) for the hybrid structure and positive ($+0.22$ V) for the cubane one (assuming that for the Fe_4S_4 systems $J_1 = 200$ cm^{-1} [36]).

Estimation of the redox potential can be carried out on the basis of the values of the average energy of spin interactions (calculated from Eq. 9). The function of the average spin energy (in J_1 parameters) versus temperature is presented in Fig. 4 and ESM, Figs. 12 and 13. The values of the redox potential, calculated as the difference of average spin energies and spin energies of the ground states for the $[Fe_4S_4]$ or $[Fe_4S_3O]$ systems, when changing the geometry of the cluster in the reduction process and at two extreme temperatures close to absolute zero and room temperature, are presented in Table 1. It should be noticed that for these temperatures the redox process takes place with preservation of the geometry of the cluster (for the hybrid-type geometry), and the redox potential is negative and relatively low (approximately a few J_1). However, this potential

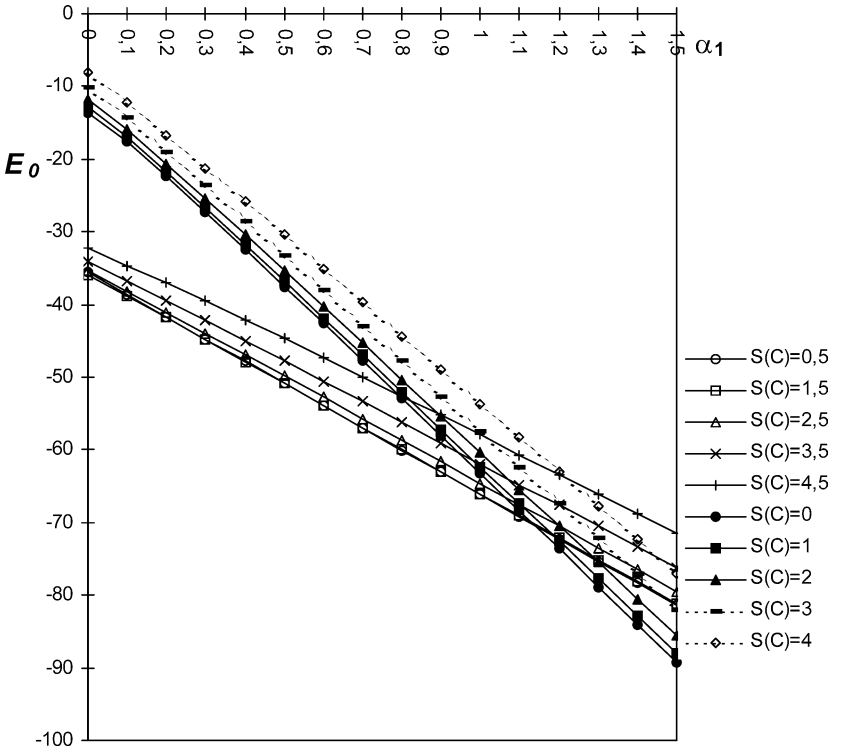

Fig. 3. Energy levels of a few of the lowest states (with resonance delocalization) in relation to the parameter α_1 for $[Fe_4S_4]^{3+}$ and $[Fe_4S_4]^{2+}$ for cubane structure.

changes to a positive value when calculated for the geometry of the cubane type. The minus sign of the potential does not change when (in the redox process) the hybrid geometry of the $[Fe_4S_4]^{3+}$ cluster changes to $[Fe_4S_4]^{2+}$ cubane geometry. This potential is positive and about twice as high as the redox potential calculated for the cubane geometry that is unchanged in the redox process. In the case where the potential is calculated as the appropriate differences in the spin state energies, we observe a slight difference in the calculated redox

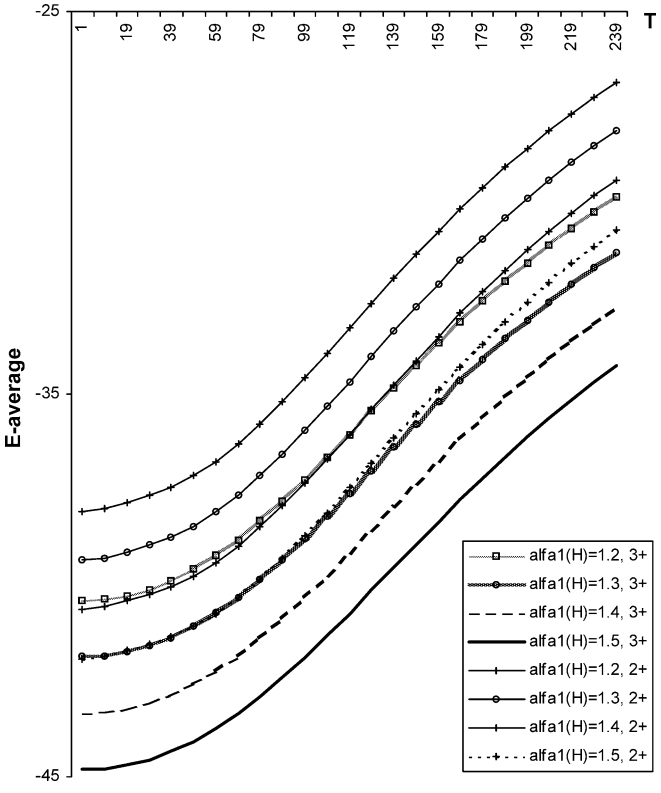

Fig. 4. The average spin energy (in J_1 units) as a function of temperature for $[Fe_4S_4]^{2+}$ and $[Fe_4S_4]^{3+}$ hybrid clusters

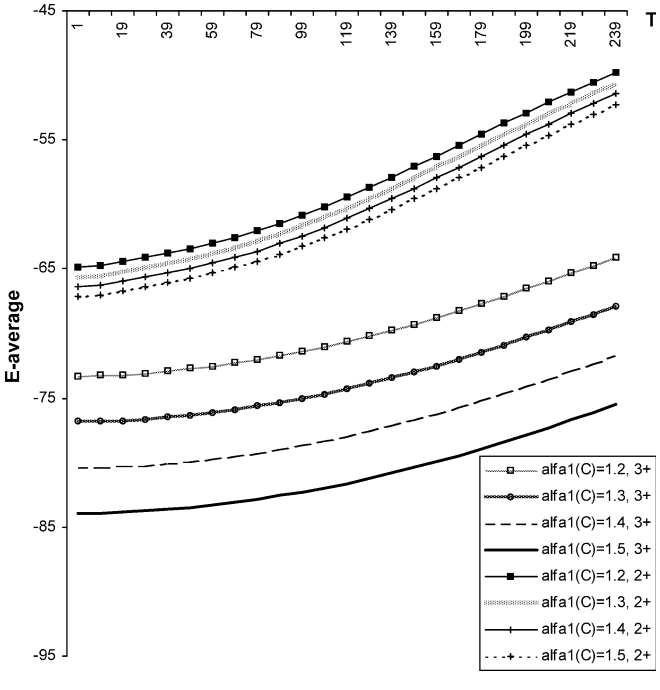

Fig. 5. The average spin energy (in J_1 units) as a function of temperature for $[Fe_4S_4]^{2+}$ and $[Fe_4S_4]^{3+}$ cubane clusters (without resonance delocalization)

potential and the redox potential calculated from the average values of spin energies.

Comparing the average spin energies calculated at room temperature, one can state that independently of other parameters the average energy values for the +3 ion are lower than those for the +2 ion (for the α_1 parameter bounded in the HiPIP area) for the hybrid structure and the difference amounts to approximately −37 mV (i.e., $-1.5J_1$). However, for the cubane structure (Fig. 5) the difference (+139 mV, i.e., $5.6J_1$) is positive and larger than for the hybrid structure. In the case considered this value agrees with the experimental one [34].

3.2 Results of the redox potential calculations for the [Fe_6S_6] system

The energy levels are presented in Figs. 6, 7, 8, 9, 10, and 11 for a few of the lowest energy states (in the case of no resonance delocalization) depending on the most important α_1 parameter (that is connected with the Heisenberg J_2 parameter describing antiferromagnetic interactions between ions of mixed valence). The α_1 value was estimated numerically only in the case of single exchange for the $[Fe_6S_6]^{5+}$ and $[Fe_6S_6]^{4+}$ superclusters of the prismane as well as the double cubane structure (for which the data can be taken from our previous publications [11, 24, 25, 26]) in various configurations of the cluster charge and the system structure. Appendix, Figs. 25–28 and 20–24 illustrate corresponding combinations in the presence of the resonance delocalization.

The dependence of the spin energy states on α_1 is presented in Fig. 6 and shows no change of the double cubane geometry. Assuming the redox potential as the difference of the energy of the +5 and +4 forms in the lowest spin states, we can conclude that in the range 0.2–0.6 this function is non-linear, then it becomes linear and approaches a nearly constant value of 13 J_1, independent of α_1. This applies, in particular, to the HiPIP systems with $\alpha_1 > 1$ (such as the previously described supercluster from *D. vulgaris*). The values of the redox potential function allow us to conclude that the J_2 parameter describing the antiferromagnetic interactions changes with the oxidation state [32].

Using Fig. 7, we will analyze the situation where the redox reaction occurs at the fixed $[Fe_6S_6]^{4+}$ and $[Fe_6S_6]^{5+}$ geometry determined as prismane. The dependence of the energy levels on α_1 in a few of the lowest $[Fe_6S_6]^{4+}$ and $[Fe_6S_6]^{5+}$ states for the prismane and double cubane structures is shown in Figs. 8 and 9. In general, for the whole range of the α_1 parameter, the states for the prismane structure are located lower and, what is more important, these states are located considerably lower than the states connected with the double cubane structure (Fig. 7). This decrease amounts to approximately $410J_1$. Therefore, the previously mentioned decrease can be mainly connected with the change of geometry of the supercluster, but only for the reduced $[Fe_6S_6]^{4+}$ form. The analysis of the data presented in Figs. 8 and 9 leads to the conclusion that for $[Fe_6S_6]^{5+}$ the states of the prismane structure are insignificantly lower than the corresponding states for the double cubane structure (approximately by $28J_1$). Summarizing, we can affirm that in the case of the $[Fe_6S_6]^{4+}$ supercluster the spin states of the lowest energy belong to the prismane-type structure.

The two highest states of the ions (ESM, Fig. 18) of charges +4 and +5 (separated in energy by approximately $13J_1$) are connected with the double cubane structure. Assuming that the redox potential is calculated as the difference in the energies of the ground spin states (with ΔZPE) for the +5 and +4 clusters, the redox potential should amount to +64 mV for $J_1 = 20\ cm^{-1}$. The experimental value of the redox potential is close to zero and for the prismatic protein from *D. vulgaris* it is +5 mV. The redox process can be modeled by higher located states (induced states) connected with the double cubane structure, whereas the lower states are associated with the structure of higher symmetry, i.e., the prismane one. Such a change in the supercluster geometry requires much more energy than in the case of the redox process.

The energy scheme obtained in the case with double exchange and in the case of the resonance delocalization does not introduce changes to the previous scheme of the energy levels (ESM, Figs. 14–17, 19) and does not change the value of the redox potential, which still amounts to around +62 mV (Table 2, ESM, Fig. 19). First of all, the energy order of the two states changes, i.e., the energy of the state with $S = 4$ for $[Fe_6S_6]^{4+}$ of the double cubane structure

Table 1. Redox potential for the [Fe4S3O] and the [Fe4S4] systems (in J_1 units). *H* and *C* denotes hybrid and cubane cluster geometries, respectively

Temperature	Geometry of the clusters	Redox potential as the difference of the average energy of the spin states (Heisenberg exchange)	Redox potential as the difference of the energy of the lowest spin states (Heisenberg exchange)
Close to absolute zero	H–H	−1.5	−4.1
	C–C	5.6	8.7
	H–C	55.2	71.4
Close to room temperature	H–H	−1.4	
	C–C	5.0	
	H–C	55.9	

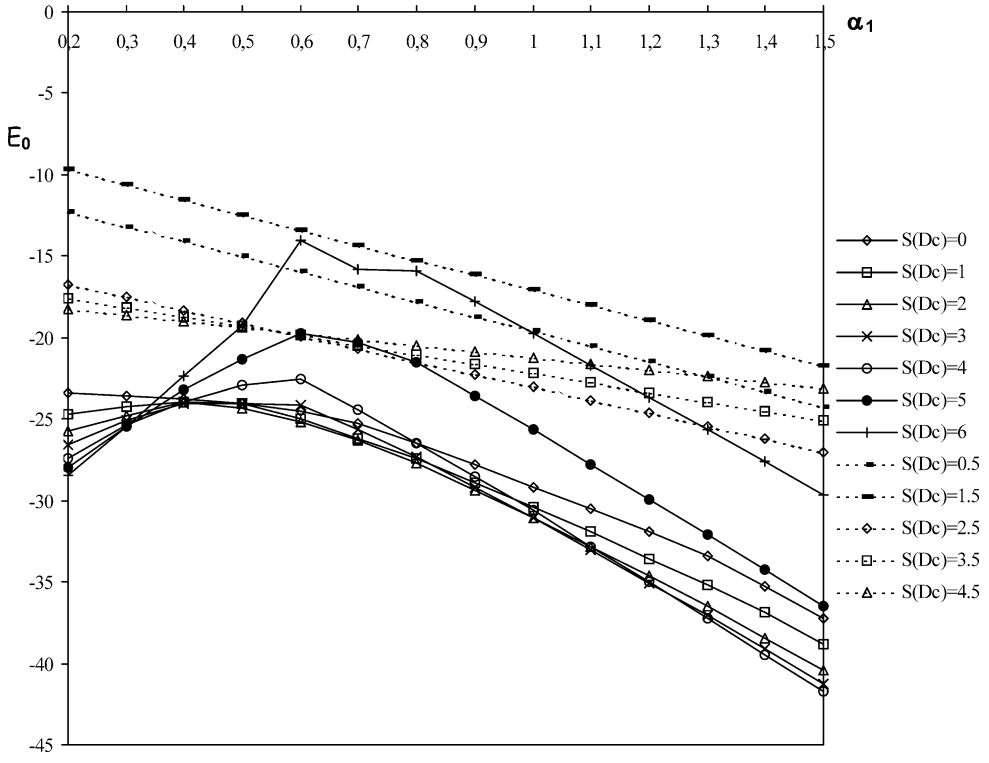

Fig. 6. Energy levels of a few of the lowest states depending on the α_1 parameter. The *continuous line* marks the states for $[Fe_6S_6]^{4+}$, whereas the *dashed line* marks the states for $[Fe_6S_6]^{5+}$, for the double cubane structure (without resonance delocalization)

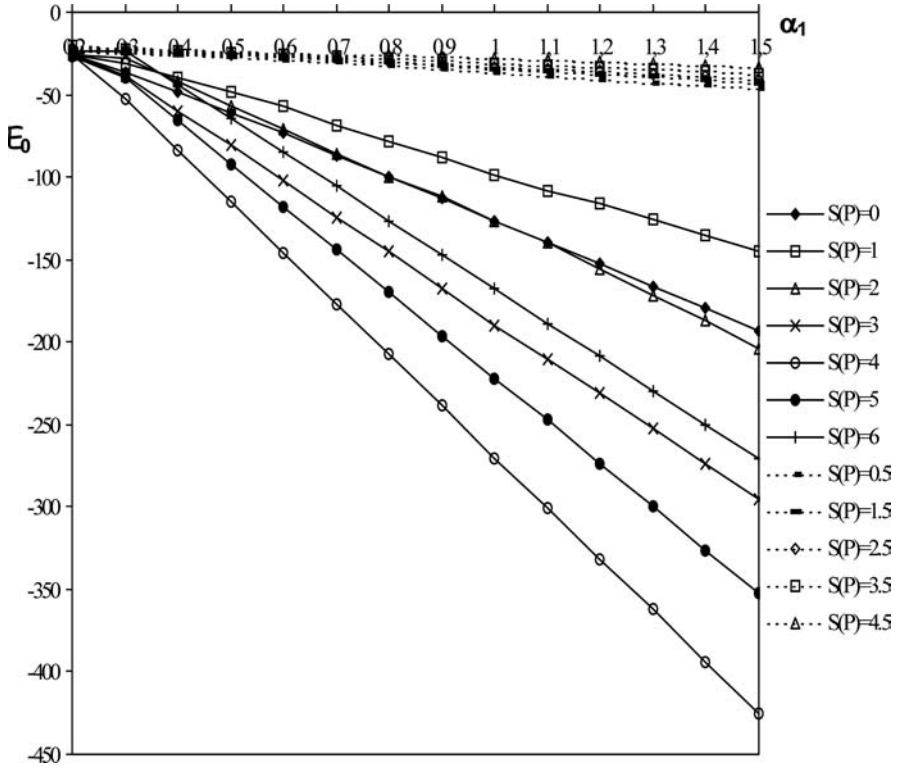

Fig. 7. Energy levels of a few of the lowest states in relation to the parameter α_1. The *continuous line* marks the states for $[Fe_6S_6]^{4+}$, whereas the *dashed line* marks the states for $[Fe_6S_6]^{5+}$, for the prismane structure (without resonance delocalization)

decreases compared with the energy of the state with $S=1/2$ for $[Fe_6S_6]^{5+}$ of the prismane geometry. The redox potential calculated at the geometry change is of the same order as in the case of the stable double cubane geometry in this process but it is negative (Table 2).

We present a function of the average spin energy (in J_1 units) versus temperature (in kelvin) for the prismane structure in Fig. 10 and ESM, Figs. 20 and 21 (calculated in accordance with Eq. 9). For the $[Fe_6S_6]^{4+}$ supercluster of the prismane type and for the single exchange and resonance delocalization, the

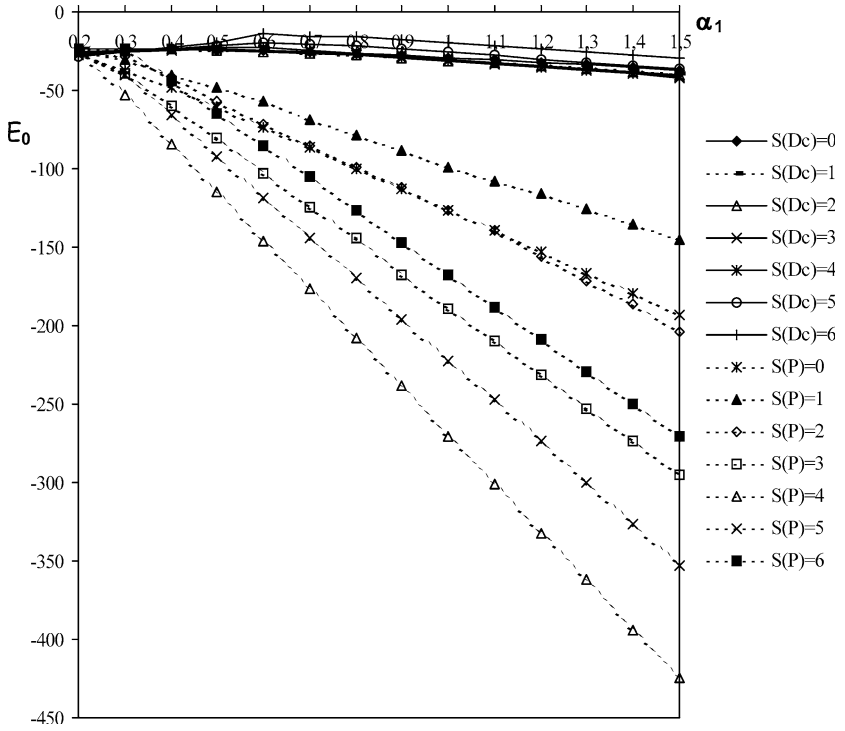

Fig. 8. Energy levels of a few of the lowest states in relation to the parameter α_1, for $[Fe_6S_6]^{4+}$ superclusters, for prismane S and double cubane S_k structures (without resonance delocalization)

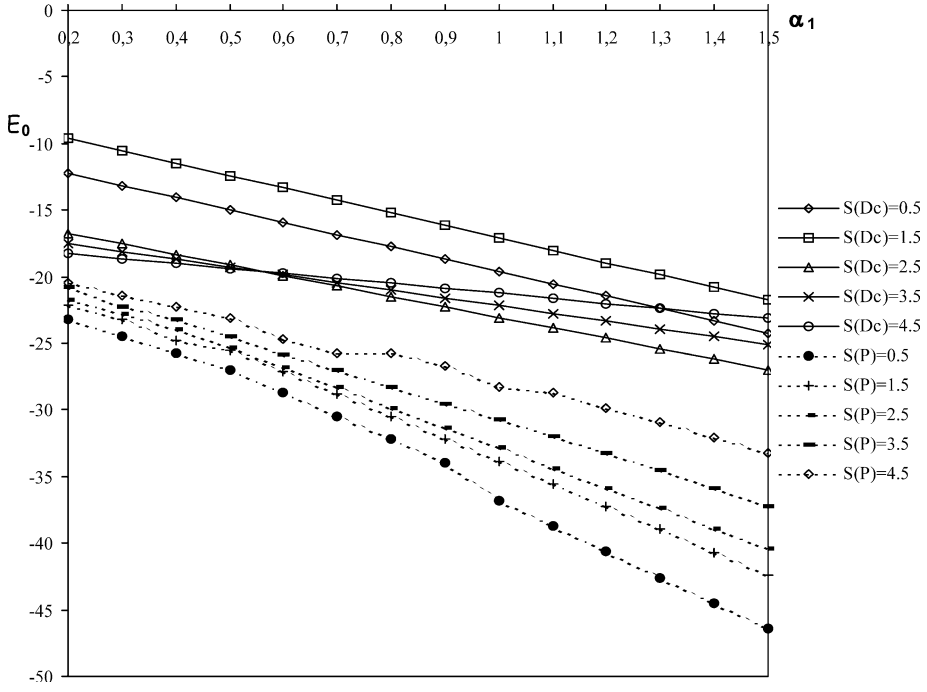

Fig. 9. Energy levelsof a few of the lowest states in relation to the parameter α_1, for $[Fe_6S_6]^{5+}$ superclusters, for prismane S and double cubane S_k structures (without resonance delocalization)

function is constant irrespective of temperature for the range of values of the parameter α_1 examined. Moreover, we can observe a slight decrease in the average-spin energy in the case of the resonance delocalization. This results from the fact that the ground state is strongly separated from excited states. In the case of the $[Fe_6S_6]^{5+}$ ion of the same geometry the function is more complicated. For $\alpha_1 = 1.2$, the linear function increases with temperature, and with increasing value of α_1 a range of temperature appears for which the function is non linear and increasing. This means that at high temperatures the ground state is not so well separated from other states and there appear occupied excited spin states. For the $+5$ and $+4$ clusters of prismane structure, the highest absolute values of the average spin energy are connected with the highest values of the α_1 parameter. Moreover, for the set of the α_1 parameters, similarly as in the case of the energy of

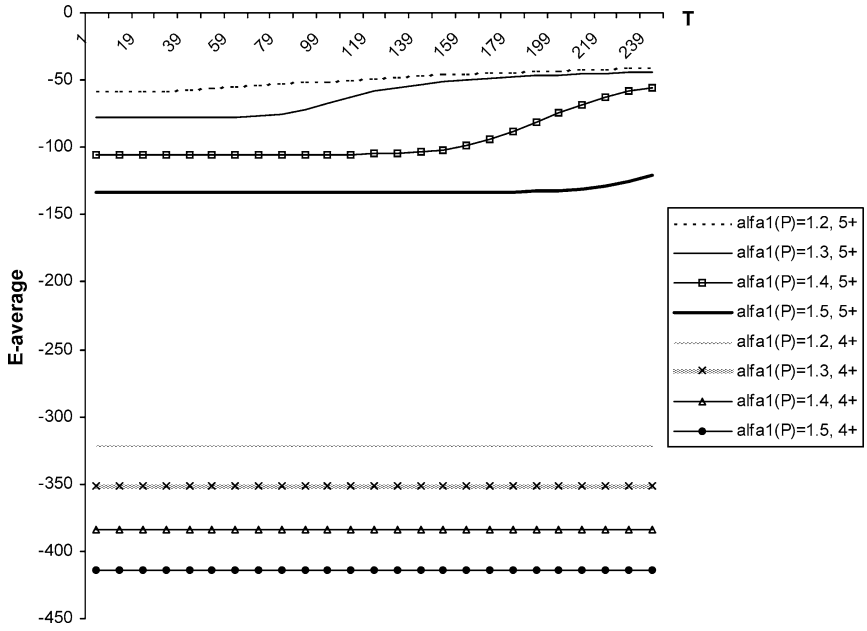

Fig. 10. The average spin energy (in J_1 units) as a function of temperature for $[Fe_6S_6]^{4+}$ and $[Fe_6S_6]^{5+}$ prismane clusters (without resonance delocalization)

the ground spin state for the superclusters, the order of the average spin energy is the same, i.e., for $[Fe_6S_6]^{4+}$ the energy is lower than for $[Fe_6S_6]^{5+}$.

We present the average spin energy for the double cubane structure in Fig. 11 and ESM, Figs. 22 and 23. For $[Fe_6S_6]^{4+}$, we observe a slight decrease in the average energy when we consider the resonance delocalization. The dependence of the average spin energy (considering resonance delocalization) on temperature for various values of the α_1 parameter is shown in ESM, Figs. 22 and 23. The dependence is non linear and similar to that for the clusters of the prismane structure, i.e., an increase of the α_1 parameter also increases the absolute value of the average spin energy in the whole range of temperature by a constant value.

In the case of $[Fe_6S_6]^{5+}$ (Figs. 10, 11), the dependence is more complicated than in the case of $[Fe_6S_6]^{4+}$. For the α_1 parameter this dependence is a non-linear function that increases with temperature. Let us note that the existing non linearity is connected with the decreasing influence of the α_1 parameter on the value of the average spin energy. This means that for high temperatures the influence of geometry and of the valence of the iron ion on the average value of the spin energy decreases. Moreover, for temperatures above140 K the average spin energy is positive, i.e., non-binding states appear at these temperatures. The resonance delocalization generally decreases the spin energy up to negative values of the average spin energy over the whole range of temperatures (from 0 K to room temperatures).

The redox potentials calculated as the differences of the average spin energies and spin energies of the ground states assuming that the cluster geometry can change in the redox process are presented in Table 2. The data collected in Table 2 allow us to interpret the dependence of the redox potential on temperature from 0 K to room temperature. One can notice that over the whole range of temperatures in the redox process with a stable geometry of the cluster (of double cubane type) and irrespective of the whether we consider resonance delocalization or not, the redox potential is positive and relatively low (tens of J_1). The situation is different when the geometry of the cluster changes in this process from the double cubane ($[Fe_6S_6]^{4+}$) to the prismane ($[Fe_6S_6]^{5+}$) one. Over the whole range of temperatures both for single exchange and for double exchange the redox potential changes to a negative value and its absolute value becomes about twice as high as the potential calculated for the case of the stable geometry.

Considering these changes, we can draw the conclusion that the oxidation process is less favorable for the hybrid and cubane geometry clusters than for the double cubane and prismane ones. Moreover, as demonstrated in the interpretation of the redox potential, it is possible to obtain conformability of the theoretical and experimental results.

Therefore, we have obtained theoretical results concerning the double cubane structure that are close to the experimental EPR and ox–redox potential results. This fact endorses the theoretical model presented here that allows us to describe properly the spin value in the ground state, the redox potential, and geometry of the active centers in proteins from *D. vulgaris*.

4 Concluding remarks

A theoretical study of the Heisenberg exchange and the double exchange (delocalization) effects in Fe–S clusters with four and six iron ions has been performed. The clusters were modeled by the Fe(II) and Fe(III) ions. Energies of the spin states were calculated numerically depending on the Heisenberg exchange J_i and the double-exchange b parameters.

Table 2. Redox potential for the $[Fe_6S_6]$ system (in J_1 units). *Dc* and *P* denote double cubane or prismane cluster geometry, respectively

Temperature	Geometry of the clusters	Redox potential as the difference of the average energy of the spin states		Redox potential as the difference of the energy of the lowest spin states	
		Heisenberg exchange	Resonance delocalization	Heisenberg exchange	Resonance delocalization
Close to absolute zero	Dc–Dc	24.6	15.0	25.9	25.2
	Dc–P	−67.5	−51.7	−33.1	−25.6
Close to room temperature	Dc–Dc	27.3	11.9		
	Dc–P	−34.7	−23.2		

Since the whole energy spectrum was calculated, the reduction process was considered. The size of the system investigated and the complicated nature of the theoretical model needed numerical calculations. It should be pointed out that although all possible Heisenberg parameters were introduced, only some of them have an influence on the calculated results.

The calculated values of the redox potential for the $[Fe_4S_3O]$ and $[Fe_4S_4]$ systems with the determined geometry of the cluster allow us to affirm the following statements:

- The calculated redox potential for the stable structure of the hybrid type, in this process, has a negative value and amounts to approximately 2 J_1, whereas for the cubane geometry the potential is positive and amounts to approximately 6 J_1.
- A change of the geometry from the cubane to the hybrid structure in the redox process considerably increases the value of the redox potential to approximately 60 J_1 (similarly as for the [Fe6S6] system).
- In all thecases discussed, an increase of temperature (also for changes of the cluster geometry) does not influence considerably the value of the calculated redox potential.

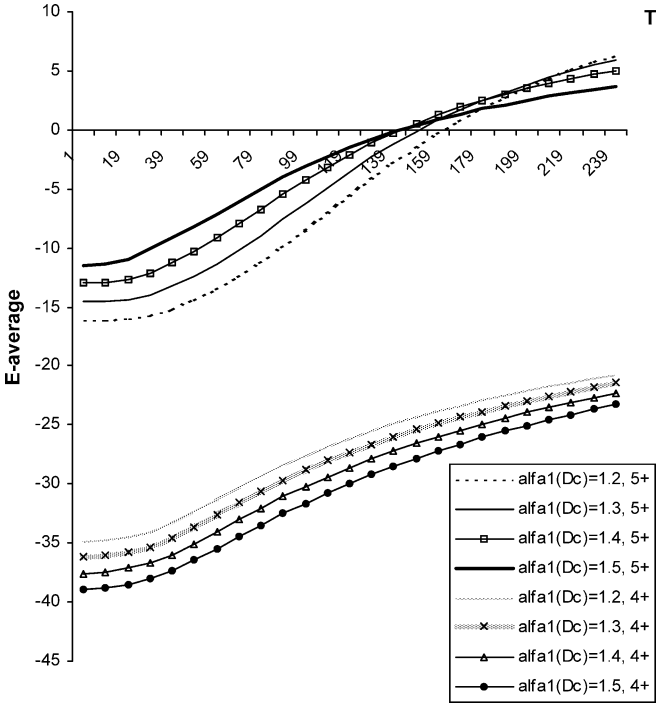

Fig. 11. The average spin energy (in J_1 units) as a function of temperature for $[Fe_6S_6]^{4+}$ and $[Fe_6S_6]^{5+}$ double cubane clusters (without resonance delocalization)

An increase in the number of iron ions allows us to examine the reciprocal influence of subsystems comprising four iron clusters each, through assuming (possibly simple) model structures with six iron superclusters, certainly maximal coupling of the spins for the prismatic protein from *D. vulgaris* may derive from eight iron superclusters. In this paper, we analyzed the influence of changing the number of iron ions in relation to the system with four ions. The analysis was carried out on the basis of the [Fe6S6] system while choosing prismane and double cubane structures. The calculated values of the redox potential allow us to draw the following conclusions:

- The lowest positive value of the redox potential was determined (for the geometry stable in the redox process) for the double cubane structure. An increase in temperature increases the value of the redox potential.
- When we consider the resonance delocalization, the redox potential decreases with increasing temperature. A change of the cluster geometry influences the redox potential, i.e., it changes from positive to a negative value of approximately −70 J_1.
- Theoretical considerations concerning the redox potential allow us to state that the best results, comparable to experimental data for *D. vulgaris*, were obtained by increasing the number of iron ions, i.e., for the compounds consisting of the four ion system $[Fe_4S_4]$ up to the six ion one $[Fe_6S_6]$, and only for the special double cubane geometry. Moreover, for this structure the increase of temperature in the redox process results in a decrease in the redox potential.

The analysis of the redox potential calculations shows that the reduction process takes place at the ''frozen'' double cubane structure and can be calculated as the difference between the average spin state energies of

the tetravalent and pentavalent superclusters. For the Heisenberg parameter $J_1 = 20$ cm^{-1}, the redox potential (close to room temperature) amounts to $+0.03$ V ($11.9J_1$). This complies with the experimental values of the redox potential for $[Fe_6S_6]^{5+/4+}$ that are close to zero.

It is generally believed that the model of the Heisenberg exchange and double exchange interactions in the Fe–S superclusters describes the physics of the system in a sufficient way. Therefore, the results can be applied in order to interpret many structural, magnetic, and redox properties of proteins possessing Fe–S active centers.

Acknowledgements We thank Valery R. Polyakov and Jacek J. Kasperczyk for critical reading of the manuscript and for valuable comments. This work was sponsored by the State Committee for Scientific Research (KBN contract no. 3T09A02815). Some of the numerical calculations were carried out at the Interdisciplinary Centre for Mathematical and Computational Modeling (Warsaw, Poland) and the Poznan Supercomputing & Networking Center (Poznań, Poland).

Appendix

Model for the hybrid system

The Hamiltonian of Eq. (1) can be transformed, excluding $\hat{H}_{\text{const}}$, into the following form for $[Fe_4S_3\,O]^{3+}$

$$\hat{H}_0 = 1/2 J_{12}\left(\hat{S}_{12}^2 - \hat{S}_1^2 - \hat{S}_2^2\right) + 1/2 J_{34}\left(\hat{S}_{34}^2 - \hat{S}_3^2 - \hat{S}_4^2\right), \tag{37}$$

$$\hat{H}_1 = {}^1/_2 J_{13}\left(\hat{S}_{13}^2 - \hat{S}_1^2 - \hat{S}_3^2\right) + {}^1/_2 J_{24}\left(\hat{S}_{24}^2 - \hat{S}_2^2 - \hat{S}_4^2\right), \tag{38}$$

and

$$\hat{H}_2 = {}^1/_2 J_{14}\left(\hat{S}_{14}^2 - \hat{S}_1^2 - \hat{S}_4^2\right) + {}^1/_2 J_{23}\left(\hat{S}_{23}^2 - \hat{S}_2^2 - \hat{S}_3^2\right) \tag{39}$$

and for $[Fe_4S_3\,O]^{2+}$

$$\hat{H}_0 = {}^1/_2 J_{12}\hat{S}_{12}^2 + {}^1/_2 J_{34}\hat{S}_{34}^2 \tag{40}$$

$$\hat{H}_1 = {}^1/_2 J_{13}\hat{S}_{13}^2 + {}^1/_2 J_{24}\hat{S}_{24}^2, \tag{41}$$

$$\hat{H}_2 = {}^1/_2 J_{14}\hat{S}_{14}^2 + {}^1/_2 J_{23}\hat{S}_{23}^2, \tag{42}$$

and

$$\begin{aligned}\hat{H}_{\text{const}} &= {}^1/_2\left[J_{12}\left(-\hat{S}_1^2 - \hat{S}_2^2\right) + J_{34}\left(-\hat{S}_3^2 - \hat{S}_4^2\right)\right.\\ &+J_{13}\left(-\hat{S}_1^2 - \hat{S}_3^2\right) + J_{24}\left(-\hat{S}_2^2 - \hat{S}_4^2\right)\\ &\left.+J_{14}\left(-\hat{S}_1^2 - \hat{S}_4^2\right) + J_{23}\left(-\hat{S}_2^2 - \hat{S}_3^2\right)\right].\end{aligned} \tag{43}$$

Eigenfunctions of the Hamiltonians in Eqs. (38) and (39) determine three different coupling schemes of four spins. Let us denote the eigenfunctions of $\hat{H}_0$, $\hat{H}_1$, and $\hat{H}_2$ (for $[Fe_4S_3O]^{3+}$) respectively as

$$\begin{aligned}\psi(S_{12}, S_{34}, S) &= |S_1 S_2(S_{12}) S_3 S_4(S_{34}) S\rangle,\\ \psi(S_{13}, S_{24}, S) &= |S_1 S_3(S_{13}) S_2 S_4(S_{24}) S\rangle,\\ \psi(S_{14}, S_{23}, S) &= |S_1 S_4(S_{14}) S_2 S_3(S_{23}) S\rangle.\end{aligned} \tag{44}$$

On the other hand, the eigenfunctions of $\hat{H}_1$ have the property

$$\begin{aligned}&\langle S_1 S_3(S_{13}) S_2 S_4(S_{24}) S \mid S_1 S_2(S_{12}) S_3 S_4(S_{34}) S\rangle\\ &\quad= \left[(2S_{12}+1)(2S_{34}+1)(2S_{13}+1)(2S_{24}+1)\right]^{1/2}\\ &\quad\times \begin{Bmatrix} S_1 & S_2 & S_{12}\\ S_3 & S_4 & S_{34}\\ S_{13} & S_{24} & S\end{Bmatrix}.\end{aligned} \tag{45}$$

Similarly the eigenfunctions of $\hat{H}_2$ can be denoted as

$$\begin{aligned}&\langle S_1 S_4(S_{14}) S_2 S_3(S_{23}) S \mid S_2(S_{12}) S_3 S_4(S_{34}) S\rangle S_1\\ &\quad= \left[(2S_{12}+1)(2S_{34}+1)(2S_{14}+1)(2S_{23}+1)\right]^{1/2}\\ &\quad\times \begin{Bmatrix} S_1 & S_2 & S_{12}\\ S_4 & S_3 & S_{34}\\ S_{14} & S_{23} & S\end{Bmatrix}.\end{aligned} \tag{46}$$

Model for the prismane system

In order to calculate the Heisenberg exchange energy, the Hamiltonian (Eq. 11) should be transformed into the following equivalent form:

$$\begin{aligned}\hat{H} &= {}^1/_2 J_1\left[\hat{S}_{156}^2 - \hat{S}_{15}^2 + \left(-\hat{S}_6^2\right)\right]\\ &+ {}^1/_2 J_2\left[\hat{S}_{1245}^2 - \hat{S}_{14}^2 - \hat{S}_{25}^2 - \hat{S}_{15}^2 - 2\hat{S}_{24}^2\right.\\ &\times +\hat{S}_{234}^2 + \left(\hat{S}_1^2 + \hat{S}_2^2 - \hat{S}_3^2 + \hat{S}_4^2 + \hat{S}_5^2\right)\Big]\\ &+ {}^1/_2 J_3\left[\hat{S}_{246}^2 - \hat{S}_{24}^2 + \left(-\hat{S}_6^2\right)\right] + {}^1/_2 J_4\\ &\times \left[\hat{S}_{135}^2 + \hat{S}_{24}^2 - \left(\hat{S}_1^2 + \hat{S}_2^2 + \hat{S}_3^2 + \hat{S}_4^2 + \hat{S}_5^2\right)\right]\\ &+ {}^1/_2 J_5\left[\hat{S}_{36}^2 + \left(-\hat{S}_3^2 - \hat{S}_6^2\right)\right] + {}^1/_2 J_6\\ &\times \left[\hat{S}_{14}^2 + \hat{S}_{25}^2 - \left(\hat{S}_1^2 + \hat{S}_2^2 + \hat{S}_4^2 + \hat{S}_5^2\right)\right],\end{aligned} \tag{47}$$

where $\hat{S}_{ijkl}^2 = \left(\hat{S}_i + \hat{S}_j + \hat{S}_k + \hat{S}_l\right)^2$, $\hat{S}_{ijk}^2 = \left(\hat{S}_i + \hat{S}_j + \hat{S}_k\right)^2$, and $\hat{S}_{ij}^2 = \left(\hat{S}_i + \hat{S}_j\right)^2$.

Since the Hamiltonian (Eq. 47) does not commute with all spin operators, it can be divided into three parts, namely, $\hat{H}_0$, $\hat{H}_1$, $\hat{H}_2$, in such a way that each part consists of operators that commute with each other within a given part, i.e.,

$$\begin{aligned}\hat{H}_0 = {}^1/_2\left[-J_1\hat{S}_{15}^2 - J_2\left(2\hat{S}_{24}^2 + \hat{S}_{15}^2\right)\right.\\ \left.+ J_4\left(\hat{S}_{246}^2 - \hat{S}_{24}^2\right) + J_4\left(\hat{S}_{135}^2 + \hat{S}_{24}^2\right)\right] + H_{\text{const}},\end{aligned} \tag{48}$$

$$\hat{H}_1 = {}^1\!/_2\left[J_2\left(\hat{S}^2_{1245} - \hat{S}^2_{14} - \hat{S}^2_{25}\right) + J_5\hat{S}^2_{36} + J_6\left(\hat{S}^2_{14} + \hat{S}^2_{25}\right)\right], \tag{49}$$

and

$$\hat{H}_2 = {}^1\!/_2\left(J_1\hat{S}^2_{156} + J_2\hat{S}^2_{234}\right), \tag{50}$$

and a rest (corresponding to a constant):

$$\begin{aligned}\hat{H}_{\text{const}} &= {}^1\!/_2\left[J_1\left(-\hat{S}^2_6\right) + J_2\left(\hat{S}^2_1 + \hat{S}^2_2 - \hat{S}^2_3 + \hat{S}^2_4 + \hat{S}^2_5\right)\right.\\ &+ J_3\left(-\hat{S}^2_6\right) + J_4\left(-\hat{S}^2_1 - \hat{S}^2_2 - \hat{S}^2_3 - \hat{S}^2_4 - \hat{S}^2_5\right)\\ &\left.+ J_5\left(-\hat{S}^2_3 - \hat{S}^2_6\right) + J_6\left(-\hat{S}^2_1 - \hat{S}^2_2 - \hat{S}^2_4 - \hat{S}^2_5\right)\right].\end{aligned} \tag{51}$$

Let us introduce a reduced dimensionless parameter $\alpha_i = \frac{J_{i+1}}{J_1}$, where $i = 1, 2, 3, 4,$ or 5.

The eigenfunctions of the total Hamiltonian (associated with the total spin S) can be presented as linear combinations of the eigenfunctions given in one of the coupling schemes (Eqs. 48, 49 or Eq. 50). We chose the eigenfunctions of $\hat{H}_0$ for this purpose. The Hamiltonian for the $[Fe_6S_6]^{4+}$ prismane system (Eq. 22) was transformed to

$$\begin{aligned}\hat{H} &= {}^1\!/_2J_1\left[\hat{S}^2_{145} - \hat{S}^2_{15} + \hat{S}^2_{236} - \hat{S}^2_{26} + \left(-\hat{S}^2_3 - \hat{S}^2_4\right)\right]\\ &+ {}^1\!/_2J_2\left[\hat{S}^2_{1256} - \hat{S}^2_{12} - \hat{S}^2_{56} - \hat{S}^2_{15} - \hat{S}^2_{26}\right.\\ &\left.+ \left(\hat{S}^2_1 + \hat{S}^2_2 + \hat{S}^2_5 + \hat{S}^2_6\right)\right]\\ &+ {}^1\!/_2J_3\left[\hat{S}^2_{246} - \hat{S}^2_{26} + \hat{S}^2_{135} - \hat{S}^2_{15} + \left(-\hat{S}^2_3 - \hat{S}^2_4\right)\right]\\ &+ {}^1\!/_2J_4\left[\hat{S}^2_{15} + \hat{S}^2_{26} + \left(-\hat{S}^2_1 - \hat{S}^2_2 - \hat{S}^2_5 - \hat{S}^2_6\right)\right]\\ &+ {}^1\!/_2J_5\left[\hat{S}^2_{12} + \hat{S}^2_{56} + \left(-\hat{S}^2_1 - \hat{S}^2_2 - \hat{S}^2_5 - \hat{S}^2_6\right)\right]\\ &+ {}^1\!/_2J_6\left[\hat{S}^2_{34} + \left(-\hat{S}^2_3 - \hat{S}^2_4\right)\right].\end{aligned} \tag{52}$$

As not all the operators in the said Hamiltonian commute with one another, it will be divided into three parts—$\hat{H}_0$, $\hat{H}_1$, $\hat{H}_2$—so that all the operators commuted with one another:

$$\begin{aligned}\hat{H}_0 =& {}^1\!/_2J_1\left(\hat{S}^2_{145} - \hat{S}^2_{15} + \hat{S}^2_{236} - \hat{S}^2_{26}\right) + {}^1\!/_2J_2\left(-\hat{S}^2_{15} - \hat{S}^2_{26}\right)\\ &+ {}^1\!/_2J_4\left(\hat{S}^2_{15} + \hat{S}^2_{26}\right) + \hat{H}_{\text{const}},\end{aligned} \tag{53}$$

$$\hat{H}_1 = {}^1\!/_2J_3\left(\hat{S}^2_{246} - \hat{S}^2_{26} + \hat{S}^2_{135} - \hat{S}^2_{15}\right), \tag{54}$$

and

$$\begin{aligned}\hat{H}_2 =& {}^1\!/_2J_2\left(\hat{S}^2_{1256} - \hat{S}^2_{12} - \hat{S}^2_{56}\right) + {}^1\!/_2J_5\left(\hat{S}^2_{12} + \hat{S}^2_{56}\right)\\ &+ {}^1\!/_2J_6\hat{S}^2_{34},\end{aligned} \tag{55}$$

where

$$\begin{aligned}\hat{H}_{\text{const}} = {}^1\!/_2&\left[J_1\left(-\hat{S}^2_3 - \hat{S}^2_4\right) + J_2\left(\hat{S}^2_1 + \hat{S}^2_2 + \hat{S}^2_5 + \hat{S}^2_6\right)\right.\\ &+ J_3\left(-\hat{S}^2_3 - \hat{S}^2_4\right) + J_4\left(-\hat{S}^2_1 - \hat{S}^2_2 - \hat{S}^2_5 - \hat{S}^2_6\right)\\ &\left.+ J_5\left(-\hat{S}^2_1 - \hat{S}^2_2 - \hat{S}^2_5 - \hat{S}^2_6\right) + J_6\left(-\hat{S}^2_3 - \hat{S}^2_4\right)\right].\end{aligned} \tag{56}$$

References

1. Wei CH, WilkeGR, Treichel PM, Dahl LF (1966) Inorg Chem 5:900
2. Harrison P (1985) Metalloproteins, parts 1, 2. MacMillan, London
3. Ogino H, Inometa S, Tobito H (1998) Chem Rev 83:2093
4. Zanello P (1988) Coord Chem Rev 83:199
5. Lowenberg W (1977) Iron–sulfur proteins, vols 1–3. Academic, New York
6. Matsubara H, Katsube Y, Wada K (1987) Iron–sulfur protein research. Springer, Berlin Heidelberg New York
7. Cammack R, Dickson DPE, Johnson CE (1977) Lovenberg W (ed) Iron–sulfur proteins, vol 3. Academic, New York, p 283
8. Pierik AJ, Hagen WR, Dunham WR, Sands H (1992) Eur J Biochem 206:705
9. Arendsen AF, Hadden J, Card G,. McAlpine AS, Bailey S, Lindley PF, Krockel M, Trautwein AX, Feiters MC, Chanock JM, Garner CD, Kooter IM, Johnson MK, Van den Berg WAM, Van Dongen WMAM, Hagen WR (1998) J Biol Inorg Chem 3:81
10. Czerwiński M, Dąbrowski J (1995) J Inorg Biochem 59:256
11. Czerwiński M, Dąbrowski J (1996) Chem Phys 213:45
12. Dąbrowski J, Czerwiński M (1997) Eur Res Conf Tomar Port 23
13. Czerwiński M, Dąbrowski J (1997) Mol Phys 90:445
14. Czerwiński M, Dabrowski J (1998) J Mol Struct (THEOCHEM) 432:15
15. Pierik AJ (1993) WAU dissertation no 1679
16. Coropceanu VP, Paldi FG, Boldyrev SI, Gamurar VJ (1997) Chem Phys 219:1
17. Bencini A, Palii AV, Ostrovsky M, Tsukerblat BS, Vyttemoeven MG (1995) Mol Phys 86:1085
18. Borras-Almenar JJ, Clemente JM, Coronado E, Palii AV, Tsukerblat BS (1996) J Chem Phys 105:6892
19. Belinskii M (1999) Chem Phys 240:303
20. Sands RH, Dunham WR (1975) Q Rev Biophys 7:443
21. Papefthymiou GC, Laskowski EJ, Frota-Pessoa S, Frankel RB, Holm RH (1982) Inorg Chem 21:1723
22. Blondin G, Girerd J–J (1990) Chem Rev 90:1359
23. Debrunner PG (1990) Hyperfine Interact 53:21
24. Matusiewicz M, Czerwiński M, Kasperczyk J, Kityk IV (1999) J Chem Phys 111:6446
25. Czerwiński M, Matusiewicz M (2001) Theor Chem Acc 106:412
26. Czerwiński M (1999) Int J Quantum Chem 72:39
27. Czerwiński M, Matusiewicz M (2002) Computer package Heisenberg mixed valence calculation, HMVC revision D1
28. Belinskii M (1993) Chem Phys 176:37
29. Noodleman L, Lovell T, Liu T, Himo F, Torres RA (2002) Curr Opin Chem Biol 6:259
30. Mouesca JM, Chen JJ, Noodleman L, Bashford D, Case DA (1994) J Am Chem Soc 116:11898
31. Li J, Nelson MR, Peng CY, Bashford D, Noodleman L (1998) J Phys Chem 102:6311
32. Noodleman L, Peng CY, Case DA, Mouesca JM (1995) Coord Chem Rev 144:1999
33. Mouesca JM, Lamotte B (1998) Coord Chem Rev 178–180:1573
34. Bian S, Cowan JA (1999) Chem Rev 190–192:1049
35. Zhou Ch, Raebiger JW, Segal BM, Holm RH (2000) Inorg Chim Acta 300–302:892
36. Antanaitis BC, Moss TH (1975) Biochim Biophys Acta 405:262